J Electroceram (2006) 17:433–437
DOI 10.1007/s10832-006-0466-0

Tunability and leakage currents of (Ba,Sr)TiO_3 ferroelectric ceramics with various additives

A. I. Dedyk · E. A. Nenasheva · A. D. Kanareykin · Ju. V. Pavlova · O. V. Sinjukova · S. F. Karmanenko

Received: 5 August 2005 / Revised: 22 August 2006 / Accepted: 23 August 2006

Abstract The $Ba_xSr_{1-x}TiO_3$ ferroelectric ceramics with magnesium (BSM) and neodymium (BSN) additives were studied. Measurements were made of tunability, dielectric losses (tan δ), leakage currents, the correlations between current-voltage $I(U)$ and capacitance-voltage $C(U)$ characteristics. $I(U)$ characteristics of high quality BSM ceramics have four regions: Ohmic, where the conductivity is linear; the horizontal region (or negative differential resistivity); the exponential dependence; and the vertical current enhancement. These BSM samples (~20% Mg additives) were distinguished by highest breakdown strength (more than 1000 V), low tan δ (less than 10^{-3} at 1 MHz) and high tunability (up to 10% at E_{max} ~2 V/μm).

Keywords Ferroelectric ceramics · BST · Magnesium additives · Tunability · Dielectric loss factor

1 Introduction

In recent years microwave high power tunable devices based on cylindrical or rectangular waveguide structures using linear and nonlinear ferroelectric ceramics have been developed for various applications [1]. Tunable ceramic waveguides, switchers, and limiters can be employed in Dielectric Loaded Accelerator structures, and are considered as an advanced prospective technology to adjust the frequency of high power high gradient dielectric accelerating structures, such as wakefield accelerators [1, 2]. The frequency is varied in the waveguide structure by placing a ferroelectric layer ($\varepsilon \sim 400$–500; thickness $t \sim 200\ \mu$m) between a layer of linear dielectric ceramic ($\varepsilon \sim 10$–100, $t \sim 2$ mm) and the outer conducting skin of the waveguide. $Ba_xSr_{1-x}TiO_3$ (BST) ceramics are the most acceptable material for this application [3], however available BST ceramics have dielectric losses (tan δ about 10^{-2} at 10 GHz) too large to be used in MW tunable devices. Accelerator applications require tunabilities in the 10–20% range, and smaller loss factors ~(3–5) $\cdot 10^{-3}$ for the same frequency. In this work we synthesized BST ferroelectric ceramics with magnesium and with neodymium additives. We studied patterned ferroelectric capacitors loaded with these materials in the radio-frequency region. The hetero-phase samples consisted of a main perovskite phase and second phase inclusions were synthesized in order to decrease the dielectric losses while maintaining the required level of tunability.

2 Experimental procedures

The barium strontium titanate solid solutions (Ba_xSr_{1-x}) TiO_3 ($x = 0.4$–0.6) were synthesized from barium and strontium titanates ($BaTiO_3$, $SrTiO_3$) [4]. The initial BST solid solution powders and Mg or Nd compounds of the required proportions were mixed and processed in a vibration mill for three hours to obtain particle size ~1 μm. Neodymium oxide was added to the ceramic compositions as a part of the linear dielectric, the solid solution of barium tgeodymium tetratitanate $BaNd_2Ti_4O_{12}$ [5]. We have studied three sample types: BSM 1 (BST + 15–20% Mg); BSM 2 (BST + 20–25% Mg),

A. I. Dedyk · J. V. Pavlova · O. V. Sinjukova ·
S. F. Karmanenko (✉)
Electrotechnical University, Saint Petersburg, 197376, Russia
e-mail: sfkarmaneko@mail.eltech.ru

E. A. Nenasheva
"GIRICOND" Research Institute, Saint Petersburg, 194223, Russia

A. D. Kanareykin
Euclid Tec Labs LLC, 5900 Harper Rd., Solon, OH 44139, USA

BSN 1 (BST + 15% Nd), and BSN 2 (BST +10% Nd). Samples of the required geometrical shape and size were prepared by hydraulic pressing. A 10% solution of polyvinyl alcohol was used as a binder. The prepared samples were sintered in air in the temperature range of 1380–1540°C during 3 h in a chamber electric furnace until zero water absorbance was obtained. The sintered samples were studied on a DRON-3 diffractometer with a Cu-K_α, Ni filter and a scanning electron microscopy (SEM).

Copper electrodes were deposited on both sides of the 500 μm thick ceramic discs using magnetron sputtering. The electrode thickness was ~3 μm. The voltage dependence of the dielectric characteristics and the leakage current were measured at 1 MHz and voltage amplitude 0.1 V. The temperature dependence of $C(T)$ and tan δ (T) were measured in the range 77–340 K. The tunability coefficient was estimated as $n = C(0)/C(U_{\max})$, where $U_{\max}$ is the maximum bias voltage applied to the electrodes. The bias electric field did not exceed 2.4 V/μm. The error of the C measurements was less than ±0.02%. The accuracy of the tan δ measurements was $\pm 2 \cdot 10^{-4}$. The error limits of the basic current measurements in Amperes ξ are $\xi = \pm(A + 0.005 I_x)$, where A is the electrometer resolution and I_x is the electric current in Amperes.

3 Results and discussion

Figure 1 shows typical microphotographs of the BSM and BSN ceramics. We observe that the BSM ceramic has the crystallites and grains of different size. Perhaps, BSM samples contain at least two phases—the basic perovskite phase (indicated by B in Fig. 1(a)) with a little Mg substitution doping and the impurity phase (I in Fig. 1(b)). The BSN ceramics has a more homogeneous structure, and the grains of small size were not found by SEM analysis (see Fig. 1(b)). Figure 1(b) has higher magnification (×6000) in comparison with Fig. 1(a) (×3000).

Figure 2 presents the capacitance-voltage characteristics of various BSM and BSN ceramics. The BSM samples had dielectric permittivity ε about 400–500, the tunability coefficient $n = 1.06$–1.11 at E $\approx$ 2 V/μm, and tan $\delta \approx 10^{-3}$. The $C(U)$ dependence was similar to a Gaussian. The hysteresis magnitude varied from several tenths of a per cent ($\Delta C/C_0 =$ 0.003–0.007 for BSM 1) up to several per cent (BSM2). The BSN samples had dielectric constants in the 500–700 range; the tunability was kept at the same level as the BSM samples; the considerable ambiguity in $C(U)$ dependence was obtained at all values of bias voltage, see Figs. 2(c) and (d). The dependence $C(U)$ had the non conventional $C \sim (U^{-2})$ parabolic shape.

The measurements of tan δ (U) dependencies exhibited an increase with applied voltage, see Fig. 3(a). Figure 3(b) shows the $C(T)$ characteristics for BSM and BSN ceramics. The temperatures of the maximal capacitance were close—185–202 K. The Curie-Weiss constant for BSM and BSN samples were $C \approx 40000$ K and $C \approx 50000$ respectively.

In spite of the comparatively low dielectric loss factor obtained on both types of ceramics, in many cases the maximal bias voltage was restricted to $U_b \sim 600$–900 V ($E = 1.1$–1.4 V/μm). Further bias voltage increases led to considerable enhancement of the conductivity. To reveal the mechanisms of ferroelectric ceramic conductivity and to optimize the electrical durability we studied the $I(U)$ dependence of different samples. The measurement results are presented in Fig. 4. The samples BSM1-1 and BSM1-2 had 20 at.% Mg and it were sintered at different temperature in the range (1400–1540)°C. The portions of the data corresponding to Ohm's law (Fig. 4(a)) were used for estimation of the sample resistance. The sample from the BSM1 group had the lowest resistance value ($R = 4 \cdot 10^{10}$ Ω) among the BSM samples, and one of the samples BSM2 had the highest resistance $R = 10^{11}\Omega$. Special attention was focused on the nonlinear parts of the $I(U)$ characteristics, which were distinguished by various dependences on applied voltage. So, the sample BSM1 had rather long horizontal part (from 80 V up to 800 V), and then exponential current increase was detected in

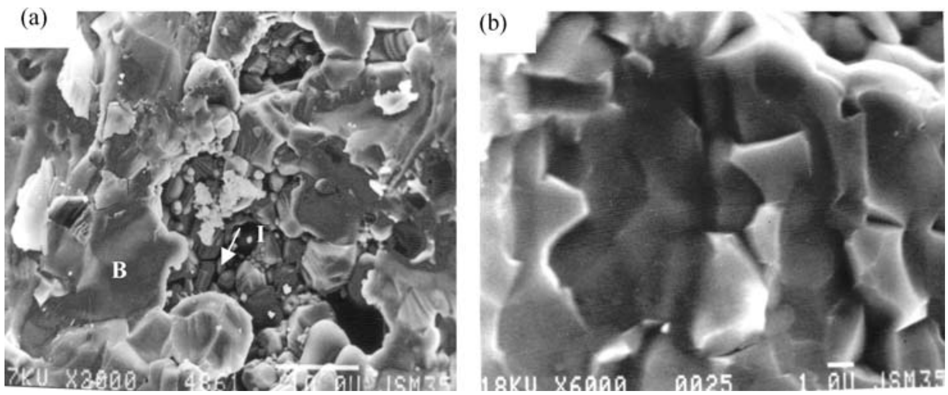

Fig. 1 SEM images of BSM (a) and BSN (b) ceramics. Figure (a) contains the designations (B)—basic phase (perovskite); and (I)—impurity, integranular phase

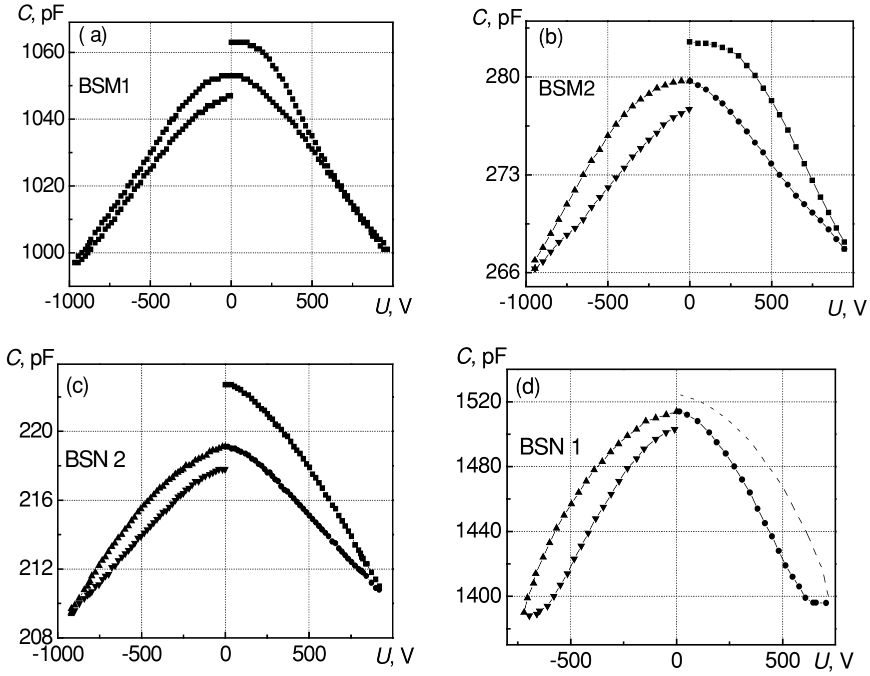

Fig. 2 The capacitance-voltage characteristics of the ceramic samples BSM1 (a); BSM2(b), BSN2 (c), and BSN1 (d)

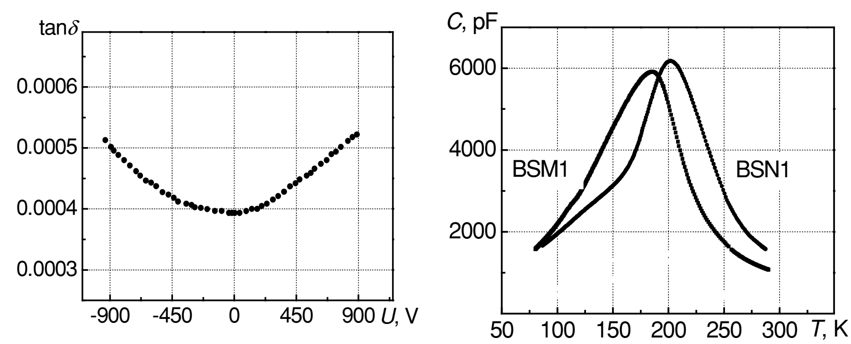

Fig. 3 The dependence of the dielectric loss factor for BSM1 ceramics on the bias voltage (a), and the temperature dependence of the ceramic capacitance (BSM1 and BSN) (b)

the region 800–900 V. This transitions to a region of practically vertical current growth were independent of bias voltage. The BSM2 sample also exhibited a horizontal region of the curve; however the length of the $I(U)$ dependence was considerably shorter. The sample BSM1 had no horizontal region, and the negative differential resistance was obviously obtained.

The current-voltage characteristics with the long horizontal region were obtained on the samples having the Gaussian shape of the $C(U)$ characteristics. The BSM samples had comparatively low hysteresis on the capacitance-voltage characteristics and visible ambiguity was revealed only at low bias voltage values (see Fig. 2(a), for the sample BSM1). The short horizontal part of the $I(U)$ dependence corresponds to considerable $C(U)$ hysteresis at every value of bias voltage (see Fig. 2(b) for the sample BSM2). In that cases, when the horizontal part on the $I(U)$ dependencies was not detected (see Fig. 4(a), the sample BSM1) or the parts with negative differential resistance were appeared (see Fig. 4(a), the sample BSM1) we obtained the essential hysteresis on the $C(U)$ characteristics and a corresponding increase of its ambiguity. Thus, BSM and BSN ceramics have these essential differences: (a) Gauss (BSM) and parabolic (BSN) character of $C(U)$ dependence; (b) the hysteresis value t$\Delta C/C \approx 3 \cdot 10^{-3}$ (BSM) and $\Delta C/C \approx 5 \cdot 10^{-2}$ BSN); (c) different shape of the $I(U)$ dependence and the resistance value on the Ohmic part of the characteristics, which is about ten times higher for BSM ceramics in comparison with BSN.

The tan $\delta(U)$ characteristic allows the possibility of making a conclusion on the loss mechanisms in the paraelectric phase [6, 7]. Most of the investigated ceramics exhibited an increasing tan $\delta(U)$ dependence (see Fig. 3(a)). As it was proposed in ref. [6] this loss factor behavior is caused by the fundamental loss character and residual polarization in a paraelectric phase. For high quality $SrTiO_3$ single crystals at 10 GHz and 77 K (pure paraelectric phase) the theoretical and experimental tan $\delta(U)$ dependences also have an increasing

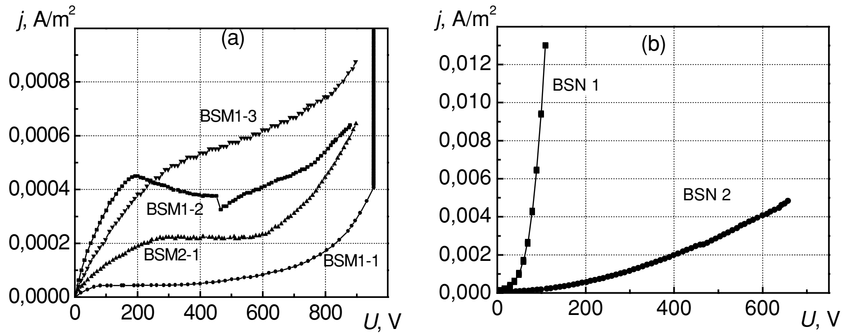

Fig. 4 Current-voltage characteristics of various BSM (a) and BSN (b) ceramic samples, which have the composition variations: BSM1-1 and BSM1-2 had 20 at.% Mg; BSM1-3 had 15 at.% Mg; BSM2-1 had 25 at.% Mg)

character. The critical temperature of the samples investigated is 100–120 K lower by comparison with the working temperature, therefore the fundamental losses can be considered as most probable loss mechanism in both ceramic types.

Let's consider the features of the $I(U)$ dependencies. The BSM samples ordinarily have four regions: Ohmic conductivity; the horizontal part or region of negative differential resistivity; the region of exponential current increase and; the region of vertical current enhancement. The samples of highest Mg concentration are characterized by the highest resistance. The horizontal $I(U)$ parts of BSM samples could be explained by rather simple inhomogenities or compensation mechanisms on the charged doping impurities. In the case of negative differential resistance the sample contains a dipole region of high electric field [8]. The estimation of the dipole layer in the ferroelectric samples can achieve 200–250 μm. Such charge inhomogenity considerably increases the hysteresis value. The horizontal parts on $I(U)$ dependencies or the negative differential resistance were observed on thin film samples [9, 10], however the model description of this effect was not accomplished. The third part on the $I(U)$ characteristics is associated with the individual energetic distribution of the charge traps. The trap activation energy for the materials studied has a wide spectrum from 0.09 up to 1.4 eV [14, 15]. The exponential part could be connected with Schottky barrier at the interface metal/dielectric [9]. The fourth part of the vertical current increase is related to the regime of the complete filling of deep traps [12]. Taking the corresponding values on the experimental $I(U)$ characteristics we can estimate the concentration p_{to} of the sticking centers, which are not filled by the electrons

$$U_{\text{CFT}} = \frac{\text{e}p_{\text{to}} L^2}{\varepsilon\varepsilon_0}, \tag{1}$$

where $\varepsilon\varepsilon_0$—dielectric permittivity; L—sample thickness. For typical BSM ceramic values, $\varepsilon = 500$, $\varepsilon_0 = 8.85 \cdot 10^{-12}$ F/m; $L = 0.5$ mm; $U_{\text{CFT}} = 1000$ V, the estimation of the concentration of acceptor sticking centers gives $p_{\text{to}} \sim 10^{20}$ m^{-3}. The practically vertical $I(U)$ dependence could be interpreted as electrical breakdown; however the electrical properties of the sample were restored after a voltage decrease.

The $I(U)$ dependencies of the BSN ceramics were characterized by a presence of two parts: the Ohmic behavior, and the part with quadratic $I(U)$ dependence. The resistance values were determined for the Ohmic part and it varied from $4 \cdot 10^9$ up to $2 \cdot 10^{10}\,\Omega$, lower than the resistance of BSM ceramics. The quadratic part of the $I(U)$ dependence corresponds to the current restricted by superfluous space charge [6, 12]. Figure 4(b) illustrates the transition from the linear $I(U)$ dependence to the quadratic one at $U_b \approx 10$ V for the sample BSN-1, and $U_b \approx 60$ V for the sample BSN-2. The comparison of the dependence of $I(U)$ and $C(U)$ of the test samples indicates that the samples with lower U_b had worse dielectric parameters. For example, the sample BSN–1 (see Fig. 2(d)) had lower resistance and parabolic dependence of the $C(U)$ characteristics. The quadratic part of the $I(U)$ characteristics of the BSN ceramics corresponds to the current restricted by the superfluous space charge. In correspondence with the theory of the current limited by this effect, the current density can be expressed [12]:

$$J = \theta\varepsilon\varepsilon_0\mu\frac{U^2}{L^3}, \tag{2}$$

where $\theta = \frac{n}{n_t}$—relation of the total concentrations of free injected and equilibrium carriers (n) to the trapped carriers concentration (n_t). Using the value of mobility of carriers taken from [11, 16] $\mu \approx 10^{-5}$ m^2/V · s, and the experimental value of electric current density $J \approx 10^{-4}$ A/m^2 and $\underline{U_b} \approx 10$ V, we estimate $\theta \approx 10^{-2}$–10^{-3}, and $n_t \approx 10^{20}$–10^{21} m^{-3} in agreement with the data in ref. [13] for the concentration of the traps in the titanates of barium and strontium. That allows determining that BSN ceramics are dielectrics with fine donor traps.

4 Conclusion

The presented investigation allows us to make a conclusion that a presence of comparatively long horizontal part on the $I(U)$ dependence testifies about high dielectric characteristics of ferroelectric ceramics. We established that investigated BSM and BSN ceramics have a bulk conductivity. The BSN ceramics with Nd additive showed lower electrical durability in comparison with BSM ceramics. In BSN ceramics the conductivity is caused by the considerable concentration of the donor traps, which is dependent on the doping concentration of neodymium. The trap distribution in BSM ceramics, perhaps, has a gradual character and the essential role belongs to the acceptor centers. In order to increase electrical durability of BSN ceramics, probably, it is necessary to apply the complex additives containing such material as Mg together with Nd.

We determined that most perspective ferroelelectric material for the Dielectric Loaded Accelerator structures is BSM1 ceramics with 20 at.% Mg additive, however further investigations and improvements of BSN ceramics could allow achieving required characteristics.

Acknowledgment This work is supported partly by the DoE SBIR program.

References

1. W. Gai, P. Schoessow, B. Cole, R. Konecny, J. Norm, and J. Simpson, *Phys. Rev. Lett.*, **6**, 2765 (1988).
2. A.M. Altmark, A.D. Kanarejkin, and I.L. Shejnman, *Tech. Phys.*, **75**, 89 (2005).
3. B.M. Goltsman, A.I. Dedyk, V.V. Lemanov, L.T. Ter–Martirosyan, and S.F. Karmanenko, *Solid State Phys.*, **38**, 2493 (1996).
4. E.A. Nenasheva, A.D. Kanareykin, N.F. Kartenko, A.I. Dedyk, and S.F. Karmanenko, *J. Electroceramics*, **13**, 235 (2004).
5. E.A. Nenasheva and N.F. Kartenko, *J. Eur. Ceram. Soc.,* **21**, 2647 (2001).
6. J.F. Scott, C.A. Araujo, B.M. Melnick, L.D. McMillan, and R. Zuleeg, *J. Appl. Phys.*, **70**, 382 (1991).
7. O.G. Vendik, L.T. Ter–Martirosyan, and S.P. Zubko, *J. Appl. Phys.*, **84**, 993 (1998).
8. A.K. Tagantsev, *Appl. Phys. Lett.*, **76**, 1182 (2000).
9. S.M. Sze, *Physics of Semiconductor Devices* (A Wiley- Interscience Publication, J. Wiley & sons, NY, 1981, volume 2), p. 450.
10. J. Celinska, V. Joshi, S. Narayan, L. McMillan, and C.A. Araujo, *Appl. Phys. Lett.*, **82**, 3973 (2003).
11. M. Davber and J.F. Scott, *J. Phys.: Cjndens. Mater.*, **16**, 515 (2004).
12. M.A. Lampert and P. Mark, *Current Injection in Solids* (Academic Press, NY and London, 1970), p. 34.
13. A.I. Dedyk, A.M. Prudan, and L.T. Ter–Martirosyan, *Solid State Phys.*, **27**, 1615 (1985).
14. G. Chanussot and G. Godefray, *C.R. Acad. Sci.*, **266 B**, 793 (1968).
15. J.A. Gorokhovatski, *The Fundamentals of Thermodepolarization Analysis* (Moscow, Nauka, 1981), p. 173.
16. D. Keroack, Y. Lepine, and J.L. Brebner, *J. Phys. C: Solid State Phys.*, **17**, 833 (1984).